1   # Supplemental Information

2   # Appendix I – Basic Model

3   *Dynamical System*

4

5   For vector population $j = 1$ (tree-hole mosquitoes) or 2 (tiger mosquitoes) we consider susceptible ($S_{L,j}$)

6   and infected ($I_{L,j}$) female larvae (where the 'larval stage' includes both the egg stage and the true larval

7   stage), as well as susceptible ($S_{M,j}$), exposed ($E_{M,j}$) and infected ($I_{M,j}$) female adults. The total larval

8   population of mosquito species j is given by $N_{L,j} = S_{L,j} + I_{L,j}$, while the total adult population is given by

9     $N_{M,j} = S_{M,j} + E_{M,j} + I_{M,j}$. For hosts, we consider susceptible (S_C), infected (I_C) and recovered (R_C)

10   classes. The total population of the host species is given by $N_C = S_C + I_C + R_C$, where N_C is defined as a

11   model parameter. Figure 1 illustrates the compartmental model for a system with two vectors (i.e., $V =$

12   2) and one host. Vector and host dynamics are described by the following equations:

13   *Host(s):*

14     $\frac{dS_C}{dt} = -\frac{S_C}{N_C}\sum_{j=1}^{V}\lambda_{CM,j}b_j I_{M,j}$ (A.1.1.a)

15     $\frac{dI_C}{dt} = \frac{S_C}{N_C}\sum_{j=1}^{V}\lambda_{CM,j}b_j I_{M,j} - hI_C$ (A.1.1.b)

16     $\frac{dR_C}{dt} = hI_C$ (A.1.1.c)

17   *Vector(s):*

18     $\frac{dS_{L,j}}{dt} = \frac{\beta_j}{K_j}\left(S_{M,j} + (1-\rho_j)I_{M,j}\right)\left(K_j - N_{L,j} - \sum_{k=1,k\neq i}^{V}\alpha_{jk}N_{L,k}\right) - w_j S_{L,j}$ (A.1.1.d)

19     $\frac{dI_{L,j}}{dt} = \frac{\beta_j}{K_j}\rho_j I_{M,j}\left(K_j - N_{L,j} - \sum_{k=1,k\neq i}^{V}\alpha_{jk}N_{L,k}\right) - w_j I_{L,j}$ (A.1.1.e)

20     $\frac{dS_{M,j}}{dt} = w_j S_{L,j} - \lambda_{MC,j}b_j S_{M,j}\frac{I_C}{N_C} - \mu_j S_{M,j}$ (A.1.1.f)

21     $\frac{dE_{M,j}}{dt} = \lambda_{MC,j}b_j S_{M,j}\frac{I_C}{N_C} - \mu_j E_{M,j} - p_j E_{M,j}$ (A.1.1.g)

22     $\frac{dI_{M,j}}{dt} = w_j I_{L,j} + p_j E_{M,j} - \mu_j I_{M,j}$ (A.1.1.h)

23   In equation (A.1.1), we assume that female mosquitoes acquire LAC by biting viremic rodents, after

24   which, females become exposed but not infectious. This reflects a latency period and corresponds to the

25   time required for within-mosquito dissemination of the virus to the salivary glands and ovaries (1). Once

26   the virus has reached the salivary glands and ovaries, transmission is possible and females move to the

27   infected class. We assume that mosquitoes with a disseminated infection remain infected for the rest of

28   their lives (2). Similar to mosquitoes, we assume that rodents become infected when they are bitten by an

29   infectious female vector. However, because rodents develop viremias within a day or two of transmission

30   (3, 4), we assume that the latency period is negligible. Following a brief viremic period, we assume that

31   rodents develop antibodies, and recover from the infection. At this point, the rodents are refractory to

32   additional re-infection. Moreover, because antibody titers remain high over a period of months (5), we

33   assume season-long immunity. For both vector-to-host and host-to-vector transmission, we assume mass-

34   action encounter rates, normalized by rodent density. This accords with the assumption of a saturated

35   functional response of mosquito biting rate to rodent density (6, 7). Finally, we assume that infected

36   female mosquitoes pass the virus to a fraction of their offspring through transovarial transmission (8, 9).

37   Equation (A.1.1) represents a single season from spring to autumn. For this reason, we do not include

38   rodent vital rates (6). Furthermore, because rodents infected with LAC are asymptomatic (4), we do not

39   consider any disease-induced mortality in the rodent population. Thus, the total number of rodents

40   remains constant throughout the season, although the number of susceptible, infected and recovered

41   rodents may change. (Including rodent demographics would require a phenologically explicit model,

42   with at least one breeding period occurring largely prior to mosquito emergence in the spring. We leave

43   this for future study, noting that, although the inclusion of explicit rodent demographics might alter

44   quantitative predictions, we do not expect significant impact on qualitative conclusions). For both the

45   tree-hole and tiger mosquito populations, we assume logistic growth. Because both mosquito species co-

46   occur in container habitats during larval development, we assume that there is interspecific competition

47   among larvae (10, 11). Like rodents, we assume that LAC infection does not induce mortality in either

48   mosquito population (12).

49   *Parameterization*

50   Table A1 summarizes parameter definitions, symbols and empirical ranges. Justification for each
51   parameter range is given below the table.
52
53   **Table A1   Parameter Definitions and Values (see Materials and Methods)***

Parameter	Sym	Range	Reference
chipmunk recovery	h	4.3-30 mo.$^{-1}$	(3, 4, 13, 14)
tree-hole mosquito to chipmunk transmission	$\lambda_{CM,1}$	0.24-0.92	(1, 13-18)
tiger mosquito to chipmunk transmission	$\lambda_{CM,2}$	0.17-0.47	(19)
chipmunk to tree-hole mosquito transmission	$\lambda_{MC,1}$	0.34-0.93	(1, 12, 13, 15-18, 20)
chipmunk to tiger mosquito transmission	$\lambda_{MC,2}$	0.18-0.94	(12, 19, 20)
tree-hole mosquito chipmunk biting rates	b_1	0.46-6.2 mo.$^{-1}$	(21-25)
	$b_{h,1}$	0.042-0.92 mo.$^{-1}$	
tiger mosquito chipmunk biting rates	b_2	0.015-0.94 mo.$^{-1}$	(26-30)
	$b_{h,2}$	0.042-2.1 mo.$^{-1}$	
tree-hole mosquito transovarial transmission	ρ_1	0.17-0.38	(8, 20, 31, 32)
tiger mosquito transovarial transmission	ρ_2	0.027-0.094	(9, 20)
tree-hole mosquito viral dissemination rate	p_1	1.9-5.0 mo.$^{-1}$	(1, 33, 34)
tiger mosquito viral dissemination rate	p_2	1.9-5.0 mo.$^{-1}$	as above (see Appendix I)
tree-hole mosquito adult mortality rate	μ_1	0.92-6.7 mo.$^{-1}$	(23, 24, 35-38)
tiger mosquito adult mortality rate	μ_2	0.93-6.9 mo.$^{-1}$	(39) and references therein
tree-hole mosquito larval maturation rate	w_1	0.55-1.66 mo.$^{-1}$	(11, 40)
tiger mosquito larval maturation rate	w_2	0.69-2.92 mo.$^{-1}$	(11, 30, 40)
tree-hole mosquito population growth rate**	r_{m1}	1.54-4.23 mo.$^{-1}$	(10, 41)
tiger mosquito population growth rate**	r_{m2}	1.08-5.19 mo.$^{-1}$	(10, 42, 43)
tree-mosquito overwintering survival	σ_1	0.92-0.96	(44)
tiger-mosquito overwintering survival	σ_2	0.78	(44)
interspecific competition on tree-hole mosquitoes	α_{12}	0.42-0.83	(10)
interspecific competition on tiger mosquitoes	α_{21}	0.25-0.73	(10)
tree-hole mosquito carrying capacity	K_1	23-1911 ha^{-1}	(24, 36, 37, 45)
tiger mosquito carrying capacity	K_2	29-2637 ha^{-1}	(10)
chipmunk/squirrel abundance	N_C	3-52 ha^{-1}	(46-49)

54 *Throughout, we assume that chipmunks serve as the amplifying host. Although grey squirrels and fox squirrels can also be amplifying hosts, less is known about
55 their ability to transmit virus to and from mosquito populations. That said, grey squirrels and chipmunks artificially infected with LAC appear to exhibit nearly
56 identical probabilities of infection, viremic periods and peak viral titers (4), suggesting that the two species are comparable in their abilities to acquire and transmit
57 virus. Moreover, although squirrels constitute a greater percentage of bloodmeal sources from LAC vectors in certain regions (22), chipmunk antibody prevalence can
58 be higher, even in nearby locations (50). This variability suggests that mosquito vectors may not prefer one host over the other, but that biting rates on the two host
59 species may be somewhat opportunistic, varying locally with relative species abundances, rather than species identity. Ultimately, we select ranges for biting rates
60 and host abundances that encompass both grey squirrels and chipmunks. Thus, while our model is largely parameterized based on chipmunks, we believe that our
61 host population could equally well comprise squirrels, chipmunks or some combination of both.

62 **oviposition rates are calculated from population growth rates as: $\beta_i = \frac{(r_{mi}+w_i)(r_{mi}+\mu_i)}{w_i}$, see below.

63

3

64　*Chipmunk recovery, h*: (a) viremias of 1-4 days for exposure via *Ae. albopictus*; viremia of 3 days for

65　exposure via tree-hole mosquitoes *Oc. triseriatus* (13); (b) viremias of 2 days for injection exposure;

66　viremias of at least 7 days for exposure via *Oc. triseriatus* (3); (c) viremias of 2-3 days for injection

67　exposure (4); (d) viremias of 2.4 (juvenile chipmunks), 2.3 (sub-adult chipmunks) and 2.4 (adult

68　chipmunks) days for exposure via *Oc. triseriatus* (14). Assuming that one month is equivalent to thirty

69　days, this gives viremic periods lasting between 0.033 mo. and 0.233 mo., or recovery rates ranging from

70　4.3 mo.$^{-1}$ to 30 mo.$^{-1}$.

71　**Oc. triseriatus** *to chipmunk transmission,* $\lambda_{CM,1}$: (a) rate of transmission from *Oc. triseriatus* to

72　suckling mice ranged from 27% to 90% for field collected mosquitoes (15); 3 of 5 chipmunks developed

73　antibodies following exposure via *Oc. triseriatus*; 67 of 99 *Oc. triseriatus* fed on chipmunks with viremia

74　levels >2.2 $Log_{10}SMICLD_{50}$/0.025 ml (i.e. at levels where any mosquito infection was observed), were

75　capable of transmitting LAC to suckling mice 28 days later – correcting for mosquito infection rates, this

76　suggests that 67 of 72.9 infected mosquitoes transmitted virus, giving a transmission rate of 0.92 (16); (c)

77　50 of 62 chipmunks exhibited viremias following exposure via *Oc. triseriatus* (14); (d) 5 of 28 *Oc.*

78　*triseriatus* that fed on chipmunks with viremia titers >2 $log_{10}PFU$/ml transmitted virus to suckling mice –

79　correcting for mosquito infection rates, this suggests that 5 of 21 infected mosquitoes transmitted virus,

80　giving a transmission rate of 0.24 (13); (e) Correcting for dissemination rates, and using *Oc. triseriatus*

81　orally infected 3 weeks prior, 75% of Walton strain, 37% of Potato Creek strain and 48% of Yankee

82　Wood strain transmitted virus to suckling mice (17); (f) 54% of TIRES-1 population, 32% of TIRES-2

83　population and 27% of TREE HOLES population transmitted virus to suckling mice; 63% of WALTON

84　strain transmitted virus to suckling mice (18); (g) 71% of *Oc. triseriatus* with disseminated infection

85　transmitted to suckling mice (1). Combining high and low transmission rates across all studies gives a

86　range from 0.24 to 0.92.

87　**Ae. albopictus** *to chipmunk transmission,* $\lambda_{CM,1}$: (a) 44% of Houston strain mosquitoes transmitted

88　LAC to suckling mice; 33% of Evansville strain mosquitoes transmitted LAC to suckling mice; 17% of

89   Indianapolis strain mosquitoes transmitted LAC to suckling mice; all mosquitoes had disseminated

90   infection (19). For these mosquitoes, rates of transmission range from 0.17 to 0.47.

91   *Chipmunk to* **Oc. triseriatus** *transmission,* $\lambda_{MC,1}$: (a) rate of infection of *Oc. triseriatus* through

92   membrane feeding ranged from 52% to 93% for field collected mosquitoes (15); (b) 3 of 4 viremic

93   chimpunks infected *Oc. triseriatus* WALTON (13); (c) 82 of 113 *Oc. triseriatus* became infected after

94   feeding on chipmunks with viremia titers >2.2 $Log_{10}SMICLD_{50}$/0.025 ml (i.e. at levels where any

95   mosquito infection was observed) (16); (d) LACV dissemination rates for *Oc. triseriatus* through

96   membrane feeding are 45% (12); (e) LACV dissemination rates for *Oc. triseriatus* through membrane

97   feeding are 86% (20) (e) LACV dissemination rates for orally infected *Oc. triseriatus* average 70% for

98   the Walton strain, 58% for the Potato Creek strain and 77% for the Yankee Woods strain (17); (f) 76% of

99   TIRES-1 population, 40% of TIRES-2 population and 56% of TREE HOLES mosquitoes developed

100   disseminated infections via artificial membrane feeder; 81% of WALTON strain, and 34% of FORT

101   WAYNE strain developed disseminated infections via artificial membrane feeder (18); (g) 57% of *Oc.*

102   *triseriatus* developed disseminated infection following membrane feeding (1). For these mosquitoes, a

103   reasonable range for rate of infection is thus 0.34 to 0.93.

104   *Chipmunk to* **Ae. albopictus** *transmission,* $\lambda_{MC,2}$: (a) 94% of Houston strain mosquitoes became

105   infected; 67% of Evansville strain mosquitoes became infected; 60% of Indianapolis strain mosquitoes

106   developed disseminated infection following membrane feeding (19); (b) LACV dissemination rates for

107   *Ae. albopictus* through membrane feeding are 18.4%. (12); (c) LACV dissemination rates for *Ae.*

108   *albopictus* through membrane feeding are 41% (20). For these mosquitoes, rate of infection thus ranges

109   from 0.18 to 0.94.

110   **Oc. triseriatus** *biting rate,* b_1: (a) In an Iowa study, 24% of total bloodmeals came from chipmunks and

111   grey squirrels (51); (b) in an Indiana study, 48-50% of bloodmeals were from chipmunks and tree

112   squirrels (25) (b) In a North Carolina study, 54% of mammalian bloodmeal sources were squirrels (29) (c)

113 the median time from emergence to blood-feeding is 2.6 days; the mean time from emergence to blood-

114 feeding is 3.08 days; the median time between oviposition and a second bloodmeal ranges from 1.6 to

115 0.79 days, depending on female age (21); (d) females can take bloodmeals as early as 3.5 days after

116 emergence; the natural gonotrophic cycle takes ~14 days (23); (e) gonotrophic cycles range from 8 days

117 to 17 days (24); To define ranges for overall biting frequency (on any vertebrate), we assume that

118 mosquitoes bite as often as every 2.6 days and as infrequently as every 18.6 days (17 day gonotrophic

119 cycle plus 1.6 days between oviposition and a second bloodmeal – notice that this implies that one blood

120 meal per gonotrophic cycle, and thus likely overestimates the period between feedings). Biting rates on

121 host species thus range from $b_1 = \frac{30}{18.6} 0.24 = 0.39$ mo.$^{-1}$ to $b_1 = \frac{30}{2.6} 0.54 = 6.2$ mo.$^{-1}$.

122 **Oc. triseriatus *human biting rate, $b_{h,1}$***: (a) In an Iowa study, 2.6% of total bloodmeals came from

123 humans (51); (b) in a North Carolina study, 8% of total bloodmeals came from humans (29). As above,

124 this suggests a human biting rate that ranges from $b_1 = \frac{30}{18.6} 0.026 = 0.042$ mo.$^{-1}$ to $b_1 = \frac{30}{2.6} 0.08 = 0.92$

125 mo.$^{-1}$.

126 **Ae. albopictus *biting rate, b_2***: (a) In a Missouri study, 7.3% of mammalian bloodmeals came from

127 squirrels (28); (b) In a North Carolina study, 11% of mammalian bloodmeal sources were squirrels (29);

128 (c) In a study across Missouri, Indiana, Illinois, Louisiana, and Florida 2.9% of bloodmeals came from

129 scuirids (27) (d) At temperatures from 20-35°C, the pre-blood meal period ranged from 4.17 days to 5.54

130 days and the duration of the gonotrophic cycle ranged from 3.5 to 8.1 days (30); (e) the period between

131 first blood feeding and oviposition was 4.85-5.76 days, depending on strain; 32.5% of females showed

132 host-seeking following a blood-meal but prior to oviposition, and this occurred between days 4-6 after the

133 first blood meals; the remainder of the females sought blood meals after ovipositing (52); (d) From Figure

134 1C in (26), the largest slope is for the Tampa population, which predicts 0.05 bloodmeals per day, while

135 the smallest slope is for the Bloomington population, which predicts 0.017 bloodmeals per day (26); To

136 define ranges for overall biting frequency (on any vertebrate), we assume that mosquitoes bite as often as

137   every 3.5 days and as infrequently as every 58.8 days (0.017 bites per day). Biting rates on host species

138   may thus range from $b_2 = \frac{30}{58.8} 0.029 = 0.015$ mo.$^{-1}$ to $b_2 = \frac{30}{3.5} 0.11 = 0.94$ mo.$^{-1}$. Because the (26)

139   study gives exceptionally low estimates for biting rates, we re-run our simulations ignoring this paper. In

140   this case, the longest time between bitings is 8.1 days, giving $b_2 = \frac{30}{58.8} 0.029 = 0.11$ mo.$^{-1}$ (see Appendix

141   VI).

142   **Ae. albopictus *human biting rate*, $b_{h,2}$**: (a) in a Missouri study, 8.2% of mammalian bloodmeals came

143   from humans (28); (b) in a North Carolina study, 24% of mammalian bloodmeal sources were human

144   (29); (c) in a study across Missouri, Indiana, Illinois, Louisiana, and Florida 4.1% of bloodmeals came

145   from scuirids (27). As above, this suggests a human biting rate that ranges from $b_2 = \frac{30}{58.8} 0.082 = 0.042$

146   mo.$^{-1}$ to $b_2 = \frac{30}{3.5} 0.24 = 2.1$ mo.$^{-1}$.

147   **Oc. triseriatus *transovarial transmission*, ρ_1**: (a) 71% of infected females transmitted to at least one

148   progeny from the third oviposition, and 46% of eggs were infected in any brood with LAC infection,

149   suggesting an overall egg infection rate of 33% (20); (b) 85% of infected females transmitted to at least

150   one progeny and 45% of eggs were infected in any brood with LAC infection for AIDL, Bluff and

151   Holmen colonies, suggesting an overall egg infection rate of 38%; 85% of infected females transmitted to

152   at least one progeny and 34% of eggs were infected in any brood with LAC infection for AD$^-$ colony,

153   suggesting an overall egg infection rate of 29%; 76% of infected females transmitted to at least one

154   progeny and 30% of eggs were infected in any brood with LAC infection for Florida colonies, suggesting

155   an overall egg infection rate of 23%; 79% of infected females transmitted to at least one progeny and 36%

156   of eggs were infected in any brood with LAC infection for Florida colonies, suggesting an overall egg

157   infection rate of 28% (31); (c) virus recovered from 28 of 92 females recovered from ovarian cycles of

158   infected females (8); (d) percent infection rates from 17% for 2nd instar larvae to 37% for adults

159   originating from the eggs of infected females (32). A reasonable range for the probability of egg infection

160   is 0.17 to 0.38.

161 **Ae. albopictus** *transovarial transmission*, ρ_2: (a) 52% of infected females transmitted to at least one

162 progeny from the third oviposition, and 18% of eggs were infected in any brood with LAC infection,

163 suggestion an overall egg infection rate of 9.4%; (b) 2.7% of adults (28 of 1022) originating from the eggs

164 of infected females were infected themselves (9). We thus suggest that the range for the probability of

165 egg infection is 0.027 to 0.094.

166 **Oc. triseriatus** *rate of viral dissemination*, p_1: (a) virus first detected in the hemolymph, salivary glands

167 and ovaries 10-13 days post infection by membrane feeding (1); (b) salivary glands are infected at 7-16

168 days after ingestion of virus (33); (c) virus detected in heads 6-10 days after infection by membrane

169 feeding (34). Assuming that one month is equivalent to thirty days, this gives dissemination periods

170 ranging in length from 0.20 mo. to 0.53 mo., or dissemination rates ranging from 1.9 mo.$^{-1}$ to 5.0 mo.$^{-1}$.

171 **Ae. albopictus** *rate of viral dissemination*, p_2: We are unaware of any studies that specifically consider

172 the rate of LAC dissemination in *Ae. albopictus*. Consequently, we set the parameter range for LAC

173 dissemination in *Ae. albopictus* equal to the range for LAC dissemination in *Oc. triseriatus*. Notice that

174 this is broadly consistent with the observation that there are no differences in viral dissemination when

175 comparing 14- and 21- day extrinsic incubation periods for LAC in the Houston strain of *Ae. albopictus*

176 (19).

177 **Oc. triseriatus** *adult mortality rate*, μ_1: For survival rate, we only use mark-release-recapture data from

178 field experiments, since mortality estimates should reflect all sources of mortality that are relevant to wild

179 populations; (a) average survival rate in a woodlot in Indiana, as calculated by the Jolly method, was 0.87

180 d^{-1}. Assuming that one month is equivalent to thirty days, this gives a mortality rate of $\mu =$

181 $-30\ln(0.87) = 4.2$ mo^{-1} (36); (b) from Figure 3 of (35), survivorship per gonadotrophic cycle, averaged

182 across all wing lengths, is 0.50 in 1985 and 0.65 in 1986 for an *Oc. triseriatus* population in Wisconsin.

183 Assuming a gonadotrophic cycle of 14 days (23), this is equivalent to mortality rates within the range $\mu =$

184 $-\frac{30}{14}\ln(0.65) = 0.92$ mo.$^{-1}$ and $\mu = -\frac{30}{14}\ln(0.5) = 1.5$ mo.$^{-1}$ (35); (c) the probability of daily survival

185   ranged from 0.917 to 0.960 for a population in Indiana. Assuming that one month is equivalent to thirty

186   days, the mortality rate ranged from $\mu = -30\ln(0.960) = 1.2$ mo.$^{-1}$ to $\mu = -30\ln(0.917) = 2.6$ mo.$^{-1}$

187   (24); (d) the daily survival rate ranged from 0.92 to 0.95 for a population in Ohio, suggesting mortality

188   rates ranging from $\mu = -30\ln(0.95) = 1.5$ mo.$^{-1}$ to $\mu = -30\ln(0.92) = 2.5$ mo.$^{-1}$ (23); (e) the daily

189   survival rate ranged from 0.93 to 0.97 for a population in Ohio, suggesting mortality rates ranging from

190    $\mu = -30\ln(0.97) = 0.91$ mo.$^{-1}$ to $\mu = -30\ln(0.93) = 2.2$ mo.$^{-1}$ (37); (f) the average daily survival rate

191   was 0.80, suggesting a mortality rate of $\mu = -30\ln(0.80) = 6.7$ mo.$^{-1}$ (38). We suggest an overall range

192   for adult mortality from 0.92 mo.$^{-1}$ to 6.7 mo.$^{-1}$

193   **Ae. albopictus *adult mortality rate*, μ_2**: (a) adult mortality rates range from 0.031 to 0.231 per day for 9

194   different mark-release-recapture experiments. We thus assume a range from 0.93 mo.$^{-1}$ to 6.9 mo.$^{-1}$ (39).

195   Notice that none of the experiments in this meta-analysis took place in North America. However, lacking

196   any other information, we use these estimates to define a range for adult mortality of *Ae. albopictus*.

197   **Oc. triseriatus *larval development rate*, w_1**: (a) The development time of *Oc. triseriatus* from first instar

198   to adult in pure cultures at low density and ~25°C was 28.2 days, while the same at high density was 47.3

199   days (40); Since we are unaware of any studies that have specifically looked at time to egg hatching in

200   *Oc. triseriatus*, we use the same range, 2.9 to 7 days, as was determined for *Ae. albopictus* (30). Note that

201   this is broadly consistent with studies of hatch rate and diapause in *Oc. triseriatus* (53). Assuming a 30

202   day month, this suggests development rates ranging between $w_2 = \frac{30}{28.2+2.9} = 0.96$ mo.$^{-1}$ and $w_2 = $

203    $\frac{30}{47.3+7} = 0.55$ mo.$^{-1}$ (b) Degree-day models in pure cultures suggest female $DD_{5.3}$ from 355 d·°C to

204   652.5 d·°C. This gives development rates ranging between $w_2 = \frac{25-5.3}{652.5} = 0.030\ d^{-1}$ and $w_2 = \frac{25-5.3}{355} = $

205    $0.055\ d^{-1}$ (i.e., 0.91 mo.$^{-1}$ and 1.66 mo.$^{-1}$) at a temperature of ~25°C (11). A reasonable range for

206   development rates is thus 0.55 mo.$^{-1}$ and 1.66 mo.$^{-1}$

Ae. albopictus *larval development rate*, w_2: (a) The development time of *Ae. albopictus* from first instar to adult in pure cultures at low density and ~25°C was 23.4 days, while the same at high density was 36.4 days (40); Assuming egg hatching times ranging from 2.9 to 7 days (30) and a 30 day month, this suggests development rates ranging between $w_2 = \frac{30}{23.4+2.9} = 1.14$ mo.$^{-1}$ and $w_2 = \frac{30}{36.4+7} = 0.69$ mo.$^{-1}$ (b) the lowest average time for egg hatching was 2.9 days, whereas under less favorable conditions, the average time for egg hatching was 7 days; depending on temperature, it took anywhere from 8.8 ± 0.6 days and 35.0 ± 0.9 days for development from first instar to adult. Assuming 30 days per month, this suggests development rates ranging between $w_2 = \frac{30}{8.8-0.6+2.9} = 2.70$ mo.$^{-1}$ and $w_2 = \frac{30}{35+0.9+7} = 0.70$ mo.$^{-1}$ (30). (c) Degree-day models in pure cultures suggest female $DD_{8.8}$ from 166.6 d·°C to 252 d·°C. This gives development rates ranging between $w_2 = \frac{25-8.8}{252} = 0.097 \, d^{-1}$ and $w_2 = \frac{25-8.8}{166.6} = 0.064 \, d^{-1}$ (i.e., between or 1.92 mo.$^{-1}$ and 2.92 mo.$^{-1}$) for temperatures ~25°C (11). A reasonable range for development rates is thus from 0.69 mo.$^{-1}$ to 2.92 mo.$^{-1}$

Oc. triseriatus *population growth rate*, r_{m1}: (a) the unlimited population growth rate is $r_{m1} = 0.080 \, d^{-1}$ (41); (b) the unlimited population growth rate in treehole fluid is $r_{m1} = 0.0514 \, d^{-1}$ while the unlimited population growth rate in tire fluid is $r_{m1} = 0.0591 \, d^{-1}$(10); (c) From the y-intercept in Figure 6 of (54), the intrinsic rate of population growth is $r_{m1} = 0.141 \, d^{-1}$ for the Illinois strain and $r_{m1} = 0.136 \, d^{-1}$ for the North Carolina strain (54). To convert from unlimited population growth rate to oviposition rate, we use the following relationship: $r_m = \frac{1}{2}\sqrt{4\beta w + (\mu - w)^2} - \frac{w+\mu}{2}$, which relates the rate of increase of the population in a single-stage model to the oviposition, maturation and adult death rates of a two-stage model. Thus $\beta = \frac{(r_m+w)(r_m+\mu)}{w}$. We assume a range for r_{m1} of 1.54 mo.$^{-1}$ to 4.23 mo.$^{-1}$. Notice that, because we select oviposition rates to match observed/estimated population growth rates, density independent larval mortality is implicitly accounted for, albeit through a lowered oviposition rate that reflects 'surviving' or 'viable' larvae, rather than egg input to the system.

230   **Ae. albopictus** *population growth rate*, r_{m2}: (a) the unlimited population growth rate is $r_{m2} = 0.06 \ d^{-1}$

231   for estimates based on survival and fecundity schedules; the unlimited population growth rate is $r_{m2} =$

232    $0.08 \ d^{-1}$ for estimates based on emergent females (42); (b) the unlimited population growth rate in

233   treehole fluid is $r_{m2} = 0.0798 \ d^{-1}$ while the unlimited population growth rate in tire fluid is $r_{m2} =$

234    $0.0904 \ d^{-1}$(10); (c) the unlimited population growth rate is $r_m = 0.0348 \ d^{-1}$ under field conditions in

235   Vero Beach, FL (55); (d) the intrinsic rate of population growth is $r = 0.095 \ d^{-1}$ to $r = 0.109 \ d^{-1}$ at

236    $22°C, r = 0.114 \ d^{-1}$ to $r = 0.130 \ d^{-1}$ at 24°C and $r = 0.153 \ d^{-1}$ to $r = 0.173 \ d^{-1}$ at 26°C.

237   Assuming a thirty day month, this gives r_{m2} between 1.08 mo.$^{-1}$ and 5.19 mo.$^{-1}$. Calculation of

238   oviposition rate from population growth rate, and assumptions related to larval mortality are the same as

239   for *Oc. triseriatus*.

240   **Oc. triseriatus** *overwintering survival*, σ_1: (a) 92% of *Oc. triseriatus* eggs survived the 1989-1990

241   winter and 96% of *Oc. triseriatus* eggs survived the 1990-1991 winter in Northern Indiana. We thus use

242   a range from 0.92 to 0.96 for *Oc. triseriatus* overwintering survival.

243   **Ae. albopictus** *overwintering survival*, σ_2: (a) 78% of *Ae. albopictus* eggs survived the 1990-1991

244   winter in Northern Indiana. Although no eggs survived the harsher 1989-1990 winter, we use the warmer

245   1990-1991 estimate for our simulations, since Northern Indiana is at the limit of the *Ae. albopictus* range.

246   Further south, for example in Appalachia, we would expect conditions more similar to the warmer of the

247   two Northern Indiana winters. We recognize, however, that 78% is likely an underestimate in southern

248   regions and may be an overestimate in northern regions. Additional simulations (not shown) suggest that

249   the model is not particularly sensitive to *Ae. albopictus* overwintering survival.

250   *Interspecific competition on* **Oc. triseriatus**, $\boldsymbol{\alpha_{12}}$: (a) Interspecific competition coefficient is given by

251    $\alpha_{12} = b_2/b_1$. In a tree-hole environment, this gives a prediction of 0.42. In a tire environment, this gives

252   a prediction of 0.83 (10); Although several other studies consider interspecific competition between *Oc.*

253   *triseriatus* and *Ae. albopictus*, the majority use study designs (e.g., replacement series) that are

254   notoriously problematic for conversion to competition coefficients (56). For this reason, we only use data

255   from the (10) study. For *Oc. triseriatus*, we assume a range of interspecific competition between 0.42 and

256   0.83.

257   **Interspecific competition on Ae. albopictus, α_{21}:** (a) In a tree-hole environment, the estimate for the

258   interspecific competition coefficient is 0.73. In a tire environment, the estimate for the interspecific

259   competition coefficient is 0.25 (10); For *Ae. albopictus*, we assume a range of interspecific competition

260   between 0.25 and 0.73.

261   **Oc. triseriatus *carrying capacity* K_1:** (a) Maximum estimates of female population size, obtained in

262   September, ranged from 905 to 1590 in Kramer's Woods (10.1 hectares) (36); (b) population estimate of

263   294 females per hectare in Northern Indiana (24); (c) estimates ranging from 44967 to 149733 females

264   per hectare in a tire yard in Indiana (45), or 6.5 times higher than the highest estimates in (24); (c)

265   estimates of female population density in a woodlot in Ohio ranged from 23 to 205 per hectare (37); (d)

266   1098 females emerged from a one-hectare site in Wisconsin in 1976 (dry year) and 1622 females emerged

267   from the same site in 1977 (wet year) (57). Because densities from the tire yard are uncharacteristically

268   high, and because the authors noted problems with their density estimates (not a closed system), we

269   assume that the factor of 6.5 for carrying capacity in tire yards versus woodlots is a better estimate than

270   the densities themselves. Overall, then, a reasonable range for carrying capacity is between 23 and 1911

271   females per hectare.

272   **Ae. albopictus *carrying capacity* K_2:** (a) carrying capacity is given by $K_i = r_{mi}/b_i$ suggesting that the

273   carrying capacity of *Ae. albopictus* is 1.24 times the carrying capacity of *Oc. triseriatus* in tree-holes and

274   1.38 times the carrying capacity of *Oc. triseriatus* in tires (10). To our knowledge, there have not been

275   any studies on *Ae. albopictus* densities at North American sites. Therefore, we use estimates for the

276   carrying capacity of *Oc. triseriatus* to determine carrying capacities for *Ae. albopictus*. This gives a range

277   between 29 and 2637 females per hectare. Notice that this is broadly similar with estimates from

278 temperate regions in Europe (58, 59), but is slightly lower than estimates from more tropical climates

279 (60).

280 **_Chipmunk density N_0:_** (a) estimated chipmunk population densities depended on habitat quality and

281 ranged from 9 to 15.7 per acre in July and from 4.7 to 11.8 per acre in September (46); (b) grey squirrel

282 densities ranged from 3 to 10 per hectare in urban parks in Baltimore, MD (47, 48, 61) (c) grey squirrel

283 densities ranged from 23 to 52 per hectare in downtown Washington, DC (49, 61). This suggests a range

284 of squirrel/chipmunk abundances from 3 to 52 per hectare.

285 *Nondimensionalization*

286 To nondimensionalize equation (A.1.1), we substitute $\tau = ht$ and scale all state variables by the total

287 rodent population. This gives:

288 *Host(s):*

289 $$\frac{ds_C}{d\tau} = -s_C \sum_{j=1}^{V} \chi_{CM,j} i_{M,j} \qquad \text{(A.1.2.a)}$$

290 $$\frac{di_C}{d\tau} = s_C \sum_{j=1}^{V} \chi_{CM,j} i_{M,j} - i_C \qquad \text{(A.1.2.b)}$$

291 $$\frac{dr_C}{d\tau} = i_C \qquad \text{(A.1.2.c)}$$

292 *Vector(s):*

293 $$\frac{ds_{L,j}}{d\tau} = \frac{\gamma_j}{\kappa_j}\left(s_{M,j} + (1-\rho_j)i_{M,j}\right)\left(\kappa_j - n_{L,j} - \sum_{k=1,k\neq i}^{V} \alpha_{jk} n_{L,k}\right) - \omega_j s_{L,j} \qquad \text{(A.1.2.d)}$$

294 $$\frac{di_{L,j}}{d\tau} = \frac{\gamma_j}{\kappa_j}\rho_j i_{M,j}\left(\kappa_j - n_{L,j} - \sum_{k=1,k\neq i}^{V} \alpha_{jk} n_{L,j}\right) - \omega_j i_{L,j} \qquad \text{(A.1.2.e)}$$

295 $$\frac{ds_{M,j}}{d\tau} = \omega_j s_{L,j} - \chi_{MC,j} s_{M,j} i_C - \upsilon_j s_{M,j} \qquad \text{(A.1.2.f)}$$

296 $$\frac{de_{M,j}}{d\tau} = \chi_{MC,j} s_{M,j} i_C - \upsilon_j e_{M,j} - \varrho_j e_{M,j} \qquad \text{(A.1.2.g)}$$

297 $$\frac{di_{M,j}}{d\tau} = \omega_j i_{L,j} + \varrho_j e_{M,j} - \upsilon_j i_{M,j} \qquad \text{(A.1.2.h)}$$

298

13

299   where $s_C = \frac{S_C}{N_C}, i_C = \frac{I_C}{N_C}, r_C = \frac{R_C}{N_C}, s_{L,j} = \frac{S_{L,j}}{N_C}, i_{L,j} = \frac{I_{L,j}}{N_C}, s_{M,j} = \frac{S_{M,j}}{N_C}, e_{M,j} = \frac{E_{M,j}}{N_C}, i_{M,j} = \frac{I_{M,j}}{N_C}$ and $\chi_{CM,j} =$

300    $\frac{\lambda_{CM,j}b_j}{h}, \chi_{MC,j} = \frac{\lambda_{MC,j}b_j}{h}, \kappa_j = \frac{K_{L,j}}{N_C}, \omega_j = \frac{w_j}{h}, \upsilon_j = \frac{\mu_j}{h}, \varrho_j = \frac{p_j}{h}, \gamma_j = \frac{\beta_{M,j}}{h}.$

301   For all reported results, we focus on the dimensional system. The non-dimensionalization scheme,

302   however, gives insight into the parameter combinations that are important for determining system

303   behavior.

Appendix II – Basic Reproduction Numbers, R_0

306   We first note that the disease free equilibrium can be obtained by setting the abundances of all disease and

307   recovered classes ($I_C, R_C, I_{L,j}, E_{M,j}, I_{M,j}$) equal to zero, and then solving for the steady state solution of

308   equation (A.1.1). For the simplest scenario, with a single disease vector, this gives:

309    $(S_C, I_C, R_C, S_L, I_L, S_M, E_M, I_M) = \left(N_C, 0, 0, \frac{K(\beta-\mu)}{\beta}, 0, \frac{wK(\beta-\mu)}{\beta\mu}, 0, 0\right)$ (A.2.1)

310   where we have dropped indices on vector parameters, since we are only considering one vector.

311   To derive R_0, we follow the method outlined in Van den Driessche and Watmough (62). Specifically, we

312   rewrite equation (A.1.1) in vector form, focusing on the infected classes, and separating into $\mathcal{F}$ all terms

313   that reflect the appearance of new infections and into $\mathcal{V}$ all remaining terms for transfer of individuals

314   between compartments. For the single-vector model, this gives:

315    $\frac{d}{dt}\begin{bmatrix} I_C \\ I_L \\ E_M \\ I_M \end{bmatrix} = \mathcal{F} - \mathcal{V},$ with $\mathcal{F} = \begin{bmatrix} \frac{S_C\lambda_{CM}bI_M}{N_C} \\ \frac{\beta\rho I_M(K-S_L-I_L)}{K} \\ \frac{S_M\lambda_{MC}bI_C}{N_C} \\ 0 \end{bmatrix}$ and $\mathcal{V} = \begin{bmatrix} hI_C \\ wI_L \\ (p+\mu)E_M \\ -wI_L - pE_M + \mu I_M \end{bmatrix}$ (A.2.2)

316   where we have again dropped vector indices. The corresponding Jacobian matrices, F and V, evaluated at

317   the disease-free equilibrium are given by:

318 $$F = \begin{bmatrix} 0 & 0 & 0 & \lambda_{CM}b \\ 0 & 0 & 0 & \rho\mu \\ \frac{\lambda_{MC}bwK(\beta-\mu)}{N_C\beta\mu} & 0 & 0 & 0 \\ 0 & 0 & 0 & 0 \end{bmatrix} \quad \text{and} \quad V = \begin{bmatrix} h & 0 & 0 & 0 \\ 0 & w & 0 & 0 \\ 0 & 0 & p+\mu & 0 \\ 0 & -w & -p & \mu \end{bmatrix}$$ (A.2.3)

319 The basic reproduction number, R_0, is defined as the dominant eigenvalue of FV^{-1} (62), thus

320 $$R_0 = \frac{\rho}{2}\left(1 + \sqrt{1 + \frac{4b^2wp\lambda_{MC}\lambda_{CM}(\beta-\mu)K}{\rho^2\mu^2\beta h(p+\mu)N_C}}\right)$$ (A.2.4)

321 *Two vectors*

322 The basic reproduction number for a system with two vectors can be derived following an identical

323 approach to the one above; however, R_0 for the two-vector model must be evaluated numerically, because

324 it is impossible to obtain a closed form solution for the disease-free equilibrium. Consequently, we write

325 the disease-free equilibrium as:

326 $$\left(S_C, I_C, R_C, S_{L,1}, I_{L,1}, S_{M,1}, E_{M,1}, I_{M,1}, S_{L,2}, I_{L,2}, S_{M,2}, E_{M,2}, I_{M,2}\right) = \left(N_C, 0, 0, S_{L,1}^*, 0, S_{M,1}^*, 0, 0, S_{L,2}^*, 0, S_{M,2}^*, 0, 0\right)$$

327 (A.2.5.a)

328 where $S_{L,1}^*$, $S_{M,1}^*$, $S_{L,2}^*$ and $S_{M,2}^*$ are defined, implicitly, as the solutions to:

329 $$\frac{\beta_1}{K_{L,1}}S_{M,1}^*\left(K_1 - S_{L,1}^* - \alpha_{12}S_{L,2}^*\right) - w_1S_{L,1}^* = 0$$ (A.2.5.b)

330 $$w_1S_{L,1}^* - \mu_1S_{M,1}^* = 0$$ (A.2.5.c)

331 $$\frac{\beta_2}{K_{L,2}}S_{M,2}^*\left(K_2 - S_{L,2}^* - \alpha_{21}S_{L,1}^*\right) - w_2S_{L,2}^* = 0$$ (A.2.5.d)

332 $$w_2S_{L,2}^* - \mu_2S_{M,2}^* = 0$$ (A.2.5.e)

333

334 As in the case of the single-vector system, we rewrite equation (A.1.1) as

15

335
$$\frac{d}{dt}\begin{bmatrix} I_C \\ I_{L,1} \\ E_{M,1} \\ I_{L,2} \\ E_{L,2} \\ I_{M,1} \\ I_{M,2} \end{bmatrix} = \mathcal{F} - \mathcal{V}, \text{ with } \mathcal{F} = \begin{bmatrix} \frac{S_C(\lambda_{CM,1}b_1 I_{M,1}+\lambda_{CM,2}b_2 I_{M,2})}{N_C} \\ \frac{\beta_1\rho_1 I_{M,1}\left(K_1-(S_{L,1}+I_{L,1})-\alpha_{12}(S_{L,2}+I_{L,2})\right)}{K_1} \\ \frac{S_{M,1}\lambda_{MC,1}b_1 I_C}{N_C} \\ \frac{\beta_2\rho_2 I_{M,2}\left(K_2-(S_{L,2}+I_{L,2})-\alpha_{21}(S_{L,1}+I_{L,1})\right)}{K_2} \\ \frac{S_{M,2}\lambda_{MC,2}b_2 I_C}{N_C} \\ 0 \\ 0 \end{bmatrix} \text{ and } \mathcal{V} = \begin{bmatrix} hI_C \\ w_1 I_{L,1} \\ (p_1+\mu_1)E_{M,1} \\ w_2 I_{L,2} \\ (p_2+\mu_2)E_{M,2} \\ -w_1 I_{L,1}-p_1 E_{M,1}+\mu_1 I_{M,1} \\ -w_2 I_{L,2}-p_2 E_{M,2}+\mu_2 I_{M,2} \end{bmatrix}$$

336 (A.2.6)

337 The corresponding Jacobian matrices, F and V, evaluated at the disease-free equilibrium are given by:

338
$$F = \begin{bmatrix} 0 & 0 & 0 & 0 & 0 & \lambda_{CM,1}b_1 & \lambda_{CM,2}b_2 \\ 0 & 0 & 0 & 0 & 0 & \frac{\beta_1\rho_1 I_{M,1}(K_1-S_{L,1}^*-\alpha_{12}S_{L,2}^*)}{K_1} & 0 \\ \frac{\lambda_{MC,1}b_1 S_{M,1}^*}{N_C} & 0 & 0 & 0 & 0 & 0 & 0 \\ 0 & 0 & 0 & 0 & 0 & 0 & \frac{\beta_2\rho_2 I_{M,2}(K_2-S_{L,2}^*-\alpha_{21}S_{L,1}^*)}{K_2} \\ \frac{\lambda_{MC,2}b_2 S_{M,2}^*}{N_C} & 0 & 0 & 0 & 0 & 0 & 0 \\ 0 & 0 & 0 & 0 & 0 & 0 & 0 \\ 0 & 0 & 0 & 0 & 0 & 0 & 0 \end{bmatrix} \text{ and}$$

339
$$V = \begin{bmatrix} h & 0 & 0 & 0 & 0 & 0 & 0 \\ 0 & w_1 & 0 & 0 & 0 & 0 & 0 \\ 0 & 0 & p_1+\mu_1 & 0 & 0 & 0 & 0 \\ 0 & 0 & 0 & w_2 & 0 & 0 & 0 \\ 0 & 0 & 0 & 0 & p_2+\mu_2 & 0 & 0 \\ 0 & -w_1 & -p_1 & 0 & 0 & \mu_1 & 0 \\ 0 & 0 & 0 & -w_2 & -p_2 & 0 & \mu_2 \end{bmatrix}$$

340 (A.2.7)

341 The basic reproduction number, R_0, is then defined as the dominant eigenvalue of FV^{-1} (62), given by

342 FV^{-1}

343
$$= \begin{bmatrix} 0 & \frac{\lambda_{CM,1}b_1}{\mu_1} & \frac{\lambda_{CM,1}b_1 p_1}{\mu_1(\mu_1+p_1)} & \frac{\lambda_{CM,2}b_2}{\mu_2} & \frac{\lambda_{CM,2}b_2 p_2}{\mu_2(\mu_2+p_2)} & \frac{\lambda_{CM,1}b_1}{\mu_1} & \frac{\lambda_{CM,2}b_2}{\mu_2} \\ 0 & \frac{\beta_1\rho_1(K_1-S_{L,1}^*-\alpha_{12}S_{L,2}^*)}{K_1\mu_1} & \frac{\beta_1\rho_1 p_1(K_1-S_{L,1}^*-\alpha_{12}S_{L,2}^*)}{K_1\mu_1(\mu_1+p_1)} & 0 & 0 & \frac{\beta_1\rho_1(K_1-S_{L,1}^*-\alpha_{12}S_{L,2}^*)}{K_1\mu_1} & 0 \\ \frac{\lambda_{MC,1}b_1 S_{M,1}^*}{N_C h} & 0 & 0 & 0 & 0 & 0 & 0 \\ 0 & 0 & 0 & \frac{\beta_2\rho_2(K_2-S_{L,2}^*-\alpha_{21}S_{L,1}^*)}{K_2\mu_2} & \frac{\beta_2\rho_2 p_2(K_2-S_{L,2}^*-\alpha_{21}S_{L,1}^*)}{K_2\mu_2(\mu_2+p_2)} & 0 & \frac{\beta_2\rho_2(K_2-S_{L,2}^*-\alpha_{21}S_{L,1}^*)}{K_2\mu_2} \\ \frac{\lambda_{MC,2}b_2 S_{M,2}^*}{N_C h} & 0 & 0 & 0 & 0 & 0 & 0 \\ 0 & 0 & 0 & 0 & 0 & 0 & 0 \\ 0 & 0 & 0 & 0 & 0 & 0 & 0 \end{bmatrix}$$

344 (A.2.8)

16

Appendix III – Elasticity Analysis of Transmission Pathways

346   We begin with equation (A.2.8), which is the next generation matrix for the full system. This gives

$$\Gamma \equiv \begin{bmatrix} 0 & \frac{\lambda_{CM,1}b_1}{\mu_1} & \frac{\lambda_{CM,1}b_1p_1}{\mu_1(\mu_1+p_1)} & \frac{\lambda_{CM,2}b_2}{\mu_2} & \frac{\lambda_{CM,2}b_2p_2}{\mu_2(\mu_2+p_2)} & \frac{\lambda_{CM,1}b_1}{\mu_1} & \frac{\lambda_{CM,2}b_2}{\mu_2} \\ 0 & 0 & 0 & 0 & 0 & 0 & 0 \\ \frac{\lambda_{MC,1}b_1S_{M,1}^*}{N_Ch} & \frac{\beta_1\rho_1(K_1-S_{L,1}^*-\alpha_{12}S_{L,2}^*)}{K_1\mu_1} & \frac{\beta_1\rho_1p_1(K_1-S_{L,1}^*-\alpha_{12}S_{L,2}^*)}{K_1\mu_1(\mu_1+p_1)} & 0 & 0 & \frac{\beta_1\rho_1(K_1-S_{L,1}^*-\alpha_{12}S_{L,2}^*)}{K_1\mu_1} & 0 \\ 0 & 0 & 0 & \frac{\beta_2\rho_2(K_2-S_{L,2}^*-\alpha_{21}S_{L,1}^*)}{K_2\mu_2} & \frac{\beta_2\rho_2p_2(K_2-S_{L,2}^*-\alpha_{21}S_{L,1}^*)}{K_2\mu_2(\mu_2+p_2)} & 0 & \frac{\beta_2\rho_2(K_2-S_{L,2}^*-\alpha_{21}S_{L,1}^*)}{K_2\mu_2} \\ \frac{\lambda_{MC,2}b_2S_{M,2}^*}{N_Ch} & 0 & 0 & 0 & 0 & 0 & 0 \\ 0 & 0 & 0 & 0 & 0 & 0 & 0 \\ 0 & 0 & 0 & 0 & 0 & 0 & 0 \end{bmatrix}$$

348   (A.3.1)

349   We define the element elasticities as

$$e_{ij} = \frac{\gamma_{ij}}{R_0}\frac{\delta R_0}{\delta \gamma_{ij}} \tag{A.3.2}$$

351   where γ_{ij} is the i,j^{th} element of Γ and $\delta R_0/\delta\gamma_{ij}$ is used to denote numerical estimation of the
352   corresponding derivative using a finite difference approximation. To group element elasticities in terms
353   of transmission processes, we re-interpret equation (A.3.1) in terms of the four different transmission
354   routes (63). This results in the following schematic, where we use m1 for tree-hole mosquitoes and m2
355   for tiger mosquitoes

356

$$\begin{bmatrix} 0 & \text{m1} \rightarrow \text{host} & \text{m1} \rightarrow \text{host} & \text{m2} \rightarrow \text{host} & \text{m2} \rightarrow \text{host} & \text{m1} \rightarrow \text{host} & \text{m2} \rightarrow \text{host} \\ 0 & \text{transovarial m1} & \text{transovarial m1} & 0 & 0 & \text{transovarial m1} & 0 \\ \text{host} \rightarrow \text{m1} & 0 & 0 & 0 & 0 & 0 & 0 \\ 0 & 0 & 0 & \text{transovarial m2} & \text{transovarial m2} & 0 & \text{transovarial m2} \\ \text{host} \rightarrow \text{m2} & 0 & 0 & 0 & 0 & 0 & 0 \\ 0 & 0 & 0 & 0 & 0 & 0 & 0 \\ 0 & 0 & 0 & 0 & 0 & 0 & 0 \end{bmatrix}$$

358

359   From this, we see that the composite elasticities should be defined as follows:

360    $e^1_{\text{horizontal}} = e_{1,2} + e_{1,3} + e_{1,6} + e_{3,1}$ (A.3.3.a)

361    $e^2_{\text{horizontal}} = e_{1,4} + e_{1,5} + e_{1,7} + e_{5,1}$ (A.3.3.b)

362    $e^1_{\text{vertical}} = e_{2,2} + e_{2,3} + e_{2,6}$ (A.3.3.c)

363    $e^2_{\text{vertical}} = e_{4,4} + e_{4,5} + e_{4,7}$ (A.3.3.d)

364

365

Appendix IV – LAC Dynamics

Equation (A.1.1) is autonomous, and specifically describes processes within a single season. To construct a multi-seasonal model, we use equation (A.1.1) to describe within-season dynamics and then apply the following discrete map to advance the system from the end of one season to the beginning of the next (64):

Host:

$$S_{C,n}(t=0) = N_C \quad \text{(A.4.1.a)} \qquad I_{C,n}(t=0) = 0 \quad \text{(A.4.1.b)} \qquad R_{C,n}(t=0) = 0 \quad \text{(A.4.1.c)}$$

Vector(s):

$$S_{M,j,n}(t=0) = 0 \qquad \text{(A.4.1.d)} \qquad\qquad S_{L,j,n}(t=0) = \sigma_j I_{L,j,n-1}(t=t_f) \qquad \text{(A.4.1.g)}$$

$$E_{M,j,n}(t=0) = 0 \qquad \text{(A.4.1.e)} \qquad\qquad I_{L,j,n}(t=0) = \sigma_j I_{L,j,n-1}(t=t_f) \qquad \text{(A.4.1.h)}$$

$$I_{M,j,n}(t=0) = 0 \qquad \text{(A.4.1.f)}$$

where n is an index denoting the year. For each simulation we begin the first season ($n=1$, $t=0$) at the disease-free equilibrium and introduce one infected adult tree-hole mosquito (Tree-hole Model, Tree-hole & Tiger Model) and/or one infected adult tiger mosquito (Tiger Model, Tree-hole & Tiger Model). We then numerically integrate the system for 4 months ($t_f = 4$). This represents one season from June through September (note that altering the length of the season has very little effect on qualitative conclusions, see Appendix VI). At the end of the season, we apply equation (A.4.1). Equations (A.4.1.a-c) indicate that, between the months of September and June, the host population suffers a complete loss of LAC protection, either through waning immunity or through adult death and juvenile replacement. Equations (A.4.1.d-h) indicate that, over this same period, all adult mosquitoes die, while remaining larvae (in this case eggs) overwinter, subject to a mortality rate, σ_j. These assumptions mean that overwintering larvae are responsible for maintaining LAC from one season to the next. Starting from the

388   new initial conditions defined by equation (A.4.1), we numerically integrate the system for another 4

389   months, representing a second season ($n = 2$). This process continues until either the infected mosquito

390   population falls below a critical density or the system reaches equilibrium. We define the critical density

391   of infected mosquitoes as $I_L + I_M < 1 \times 10^{-6}$ ha^{-1} (Tree-hole Model, Tiger Model) or $I_{L,1} + I_{M,1} + I_{L,2} +$

392    $I_{M,2} < 1 \times 10^{-6}$ ha^{-1} (Tree-hole & Tiger Model). For each system, we define equilibrium as the

393   condition where the absolute change in the abundance of infected mosquitoes from one year to the next

394   falls below 1×10^{-6} ha^{-1}.

395   To classify LAC as persistent in any given simulation, we require that the number of infected mosquitoes

396   at the end of the season exceed $I_M + I_L > 1 \times 10^{-2}$ (Tree-hole Model, Tiger Model) or $I_{M,1} + I_{L,1} +$

397    $I_{M,2} + I_{L,2} > 1 \times 10^{-2}$ (Tree-Hole & Tiger Model). We select this threshold because simulations suggest

398   that the end-of-season infected mosquito abundance is bimodal, with one peak below our tolerance for

399   continuing simulations (1×10^{-6}) and one peak between 1-2 ha.$^{-1}$. The lower peak contains the systems

400   where LAC is decreasing to extinction, while the upper peak contains the systems where LAC persists.

401   The threshold 1×10^{-2} lies between these two peaks for all vector combinations (see Figure A1). Figure

402   A2 shows a typical output from one dynamical simulation of the Tree-hole & Tiger Model.
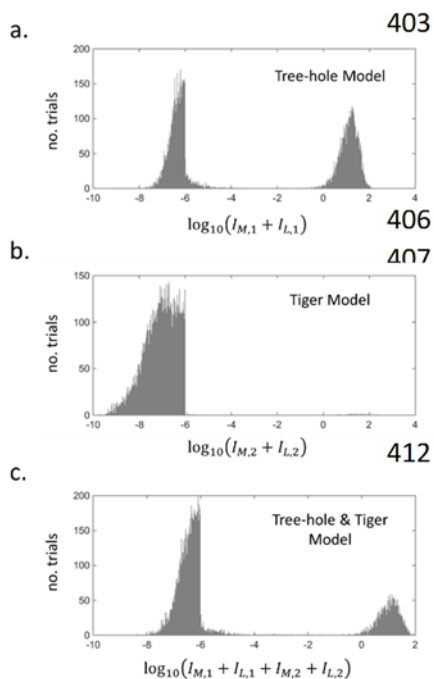
Figure A1   Histograms showing the frequency of different infection rates based on LHS analysis of (a) the Tree-hole Model (b) the Tiger Model and (c) the Tree-hole & Tiger Model. Each panel shows the results from 10,000 randomly selected parameter sets sampled over the ranges in Table A1. Notice that the threshold value of 10^{-2} lies between the two peaks of the bimodal distributions in all three models.

415
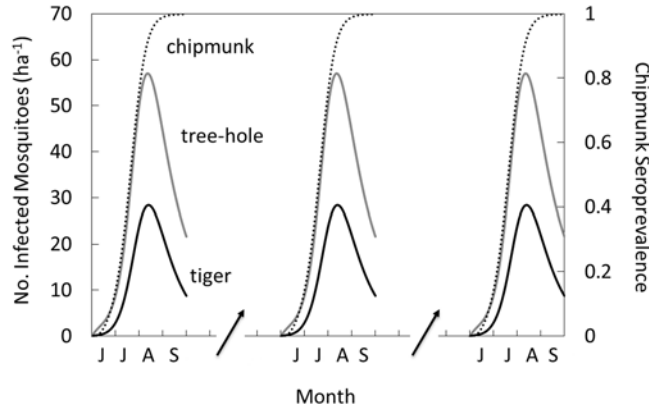
Figure A2 Output from one dynamic simulation of the Tree-hole & Tiger Model, showing the
abundances of infected tree-hole mosquitoes (solid grey) and tiger mosquitoes (solid black) and host
seroprevalence (dashed black). Parameters for this simulation were: $\lambda_{MC,1} = 0.56$, $\lambda_{MC,2} = 0.85$, $\lambda_{CM,1} = 0.86$, $\lambda_{CM,2} = 0.45$, $\mu_1 = -\log(0.32)$, $\mu_2 = -\log(0.29)$, $r_{M,1} = 2.53$, $r_{M,2} = 2.00$, $\rho_1 = 0.24$, $\rho_2 = 0.09$, $K_1 = 1545$, $K_2 = 1969$, $w_1 = 0.96$, $w_2 = 2.21$, $b_1 = 3.29$, $b_2 = 0.35$, $p_1 = 4.85$, $p_2 = 4.04$, $\alpha_{12} = 0.77$, $\alpha_{21} = 0.68$, $h = 4.35$, $N_C = 39$, $\sigma_1 = 0.95$, $\sigma_2 = 0.78$.

422

423   To account for the possibility that the apparent increase in LAC in Appalachia is a result of more human

424   infections, rather than more infections in wildlife settings, we use the dynamical model to estimate the

425   rate of disease transmission to humans. Specifically, we multiply the number of infected mosquitoes by

426   their biting rates on human hosts (see Table A1) and then consider peak rates of transmission to humans.

427   This allows us to study the potential of the tiger mosquito to act as a bridge vector.

428

429   Appendix V – Latin Hypercube Sampling and PRCC

430   *LHS Matrices*

431   We use Latin Hypercube Sampling (LHS) (65) to explore model behavior over the parameter space

432   defined by Table A1. To generate LHS matrices, we assume uniform distributions over all parameters

433   except for mortality rate. For mortality rate, we assume an exponential distribution because most

434   estimates of mortality rate come from survival measurements. Assuming a uniform distribution over

435   survival rates leads to an exponential distribution over mortality rates. In addition, this assumption helps

436   to prevent the single low estimate for survival (see Appendix I) from skewing parameter space towards

437   artificially high mortalities.

438   The only other complication with our LHS analysis is correlation between the tree-hole mosquito carrying

439   capacity and the tiger mosquito carrying capacity. In particular, because the breeding requirements of the

440   two species are similar, regions with large numbers of natural and artificial containers should be capable

441   of supporting high densities of either mosquito species. Consequently, we do not select tiger mosquito

442   carrying capacities independently from tree-hole mosquito carrying capacities. Instead, we first select

443   values for the tree-hole mosquito carrying capacities, and then determine the tiger mosquito carrying

444   capacities using a scale factor ranging from 1.24 to 1.38 (see Appendix I). We use tree-hole mosquito

445   carrying capacities as the standard, since these have been estimated empirically. In contrast, the carrying

446   capacities of tiger mosquitoes have not been so estimated, at least in North America.

447   *LHS Results*

448   Tables A2 and A3 show LHS results for 10,000 estimates of R_0 based on the parameter ranges in Table

449   A1 and each of the Tree-hole Model, the Tiger Model, and the Tree-hole and Tiger Model.

450   **Table A2 Summary statistics for R_0 and mosquito abundances based on LHS analysis**

	Tree-hole Model	Tiger Model	Tree-hole and Tiger Model*
R_0, the Basic Reproduction Number			
Mean	1.9	0.28	1.1 (1.2)
Median	1.3	0.19	0.73 (0.85)
Maximum	30	6.1	22 (22)
Minimum	0.19	0.03	0.03 (0.18)
Trials with $R_0 > 1$	60%	3%	37% (42%)
Mosquito Abundance (ha^{-1})			
Mean	600	1223	1262 (1258)
Median	475	927	1013 (1020)
Maximum	2906	7210	7094 (7094)
Minimum	2.6	6.2	10.2 (10.2)

451   *( ) is used to denote summary statistic over the subset of parameter combinations that gave equilibrium coexistence
452   between tree-hole and tiger mosquitoes. For these systems, mosquito abundance reflects the *total* density of
453   mosquitoes, including mosquitoes of both species.

454 **Table A3 Summary statistics for mosquito competitive interactions based on LHS analysis of the Tree-Hole**
455 **and Tiger Model**

	Tree-hole Mosquitoes	Tiger Mosquitoes
Competitive exclusion		
Trials where species is excluded	14%	0.03%
Trials with species coexistence	86%	
Trials with coexistence*		
Mean abundance (ha^{-1})	228	1030
Median abundance (ha^{-1})	149	759
Mean reduction due to competition	63%	16%
Median reduction due to competition	62%	13%
Mean percentage of mosquitoes	22%	78%
Median percentage of mosquitoes	17%	83%

457 *notice that these numbers reflect the mean and median of the abundance reductions or percentages, rather than the
458 reductions or percentages of the mean or median abundances

459

460 *PRCC Analysis*

461 PRCCs are determined for each of the parameters in Table A1 against R_0. First we define a $\aleph \times Y$ matrix,

462 where the $\aleph$ rows represent each of the $\aleph$ LHS trials and the Y columns store the ordinal ranks for each of

463 the Y model parameters across each of the $\aleph$ LHS runs. We then add to this matrix one additional

464 column, $Y + 1$, that contains the ordinal ranks of R_0 for each of the $\aleph$ LHS runs. If any two of the input

465 parameters have exactly the same ranking for every run, then only one of the parameters is used to

466 calculated PRCCs. For each LHS run, we thus have the set $\left(y_{i,1}, y_{i,2}, \ldots y_{i,Y+1}\right)$, where the first Y

467 numbers are the ordinal ranks of the model parameters for run i and the last number is the ordinal rank of

468 R_0 for run i. Next, we define a $Y + 1 \times Y + 1$ symmetric matrix Z, with elements z_{ij}

469
$$z_{ij} = \frac{\sum_{f=1}^{\aleph}(y_{f,i}-\varsigma)(y_{f,j}-\varsigma)}{\sqrt{\sum_{f=1}^{\aleph}(y_{f,i}-\varsigma)^2 \sum_{g=1}^{\aleph}(y_{g,j}-\varsigma)^2}}$$
(A.5.1)

470 where $\varsigma = (1 + N)/2$ is the average rank. From Z we define Q as its inverse

471
$$Q = [q_{ij}] = Z^{-1}$$
(A.5.2)

472 The PRCC between R_0 and input parameter i is then given by

473
$$PRCC_i = \frac{-q_{i,Y+1}}{\sqrt{q_{ii}q_{Y+1,Y+1}}}$$
(A.5.3)

474 The significance of a non-zero PRCC can then be tested by computing t_i

475
$$t_i = PRCC_i\sqrt{\frac{N-2}{1-PRCC_i}}$$
(A.5.4)

476

477 *PRCC Results*

478 Table A4 shows PRCC values, along with p-values, for all parameters in our model based on 10,000

479 dynamic simulations of the Tree-hole Model, the Tiger Model, and the Tree-hole & Tiger Model.

480
481 **Table A4 PRCC analysis for R_0**

Parameter	PRCC Tree-hole & Tiger Model (Tree-hole Model)	p-value Tree-hole & Tiger Model (Tree-hole Model)	Parameter	PRCC Tree-hole & Tiger Model (Tiger Model)	p-value Tree-hole & Tiger Model (Tiger Model)
tree-hole mosquito parameters			tiger mosquito parameters		
$\lambda_{MC,1}$	0.1724 (0.3491)	0 (0)	$\lambda_{MC,2}$	0.0691 (0.4346)	4.4×10^{-13} (0)
$\lambda_{CM,1}$	0.2136 (0.4288)	0 (0)	$\lambda_{CM,2}$	0.0589 (0.3034)	6.6×10^{-10} (0)
$-\log(\mu_1)$	0.5953 (0.8079)	0 (0)	$-\log(\mu_2)$	-0.0022 (0.7617)	0.41 (0)
$r_{M,1}$	0.2161 (0.0424)	0 (7.5×10^{-6})	$r_{M,2}$	-0.3229 (0.1077)	0 (0)
ρ_1	0.1064 (0.1262)	0 (0)	ρ_2	0.0269 (0.2953)	0.0032 (0)
K_1	0.1474 (0.7205)	0 (0)	K_2	-0.1120 (0.6617)	0 (0)
w_1	0.0499 (0.3493)	1.6×10^{-7} (0)	w_2	0.2163 (0.3506)	0 (0)
b_1	0.6150 (0.8617)	0 (0)	b_2	0.1989 (0.8558)	0 (0)
p_1	0.0616 (0.1239)	1.1×10^{-10} (0)	p_2	-0.0023 (0.1013)	0.41 (0)
α_{12}	-0.5901	0	α_{21}	0.0647	1.1×10^{-11}

Parameter	PRCC Tree-hole & Tiger Model (Tree-hole Model, Tiger Model)	p-value Tree-hole & Tiger Model (Tree-hole Model, Tiger Model)
chipmunk parameters		
h	-0.3798 (-0.5542, -0.4894)	0 (0,0)
N_C	-0.4716 (-0.6537, -0.5863)	0 (0,0)

482

483

484

485

486

Appendix VI – Summary Statistics for Alternate Scenarios

Because the minimum tiger mosquito biting rate is influenced by one particularly low estimate, we consider an additional analysis with a higher lower bound (0.11) on this parameter. Table A5 presents results for this analysis. Comparing Table A5 with Table 1 from the main text shows that the qualitative predictions of the model remain the same, even at a higher minimum tiger mosquito biting rate. In particular, the presence of the tiger mosquito is still not sufficient to explain the dramatic increase in LAC in Appalachia.

To explore the role of season length, we consider simulations with both shorter and longer seasons. Tables A6 and A7 presents results for dynamic simulations of the Tree-hole Model, the Tiger Model and the Tree-hole & Tiger Model for a system with a three month mosquito breeding season and a system with a five month mosquito breeding season. Comparing Tables A5 and A6 with Table 1 from the main text shows, again, that qualitative model predictions remain the same. Specifically, the tiger mosquito still has a dampening effect on LAC transmission. In general, shorter seasons result in fewer scenarios where LAC persists. However, when LAC does persist in systems with shorter seasons, many metrics of disease transmission are, on average, higher.

509 **Table A5 Summary statistics* for epidemiological metrics based on LHS analysis of the full dynamic model**
510 **with a higher lower bound on tiger mosquito biting rates; all metrics beyond the first row are only calculated**
511 **for the subset of simulations that gave infected mosquitoes**

	Tree-hole Mosquitoes	Tiger Mosquitoes	Tree-hole and Tiger Mosquitoes*
Parameter Sets with LAC Persistence	46%	0.26%	24%
End of Season Host Seroprevalence Rate			
Mean	88%	76%	84%
Median	99%	82%	98%
Maximum	100%	100%	100%
Mid-Season Host Seroprevalence Rate			
Mean	65%	16%	18%
Median	73%	11%	12%
Maximum	100%	68%	99%
Peak No. Infected Mosquitoes (ha^{-1})			
Mean	32	61	24
Median	23	52	17
Maximum	281	199	228
Peak Mosquito Infection Rate			
Mean	4.6%	1.8%	1.9%
Median	3.6%	1.4%	1.3%
Maximum	28%	4.6%	18%
Average Mosquito Infection Rate			
Mean	2.0%	0.52%	0.81%
Median	1.6%	0.45%	0.58%
Maximum	14%	1.5%	7.4%
Max. Human Transmission (mo^{-1}person^{-1}ha^{-1})			
Mean	16	62	14
Median	8.7	44	8.6
Maximum	174	257	269
Timing of Peak Human Transmission			
Mean	8/14	9/19	8/22
median	8/10	9/30**	8/20
Earliest	6/24	8/15	6/29
Latest	9/30**	9/30**	9/30**
End of Season Egg Infection Rates			
Mean	0.64%	0.07%	0.28%
Median	0.50%	0.07%	0.20%
Maximum	5.7%	0.20%	2.2%

512 *As in the main paper, we do not report minimum values
513 **In these systems, the abundance of infected mosquitoes was still increasing at the end of the season. This
514 indicates that infection rates do not slow prior to the decline in mosquitoes at the end of the summer.
515

516 **Table A6 Summary statistics for epidemiological metrics based on LHS analysis of the full dynamic model**
517 **assuming a 3 month mosquito breeding season; all metrics beyond the first row are only calculated for the**
518 **subset of simulations that gave infected mosquitoes**

	Tree-hole Model	Tiger Model	Tree-hole and Tiger Model*
Parameter Sets with LAC Persistence	40%	0.09%	19%
End of Season Host Seroprevalence Rate			
Mean	88%	82%	84%
Median	99%	92%	97%
Maximum	100%	100%	100%
Mid-Season Host Seroprevalence Rate			
Mean	74%	32%	24%
Median	88%	29%	17%
Maximum	100%	70%	99%
Peak No. Infected Mosquitoes (ha^{-1})			
Mean	34	58	26
Median	25	62	19
Maximum	280	92	180
Peak Mosquito Infection Rate			
Mean	5.0%	2.2%	2.2%
Median	4.0%	2.0%	1.6%
Maximum	29%	4.1%	14%
Average Mosquito Infection Rate			
Mean	2.3%	0.54%	0.96%
Median	1.9%	0.42%	0.66%
Maximum	17%	1.4%	7.6%
Max. Human Transmission (mo^{-1}person^{-1}ha^{-1})			
Mean	16	60	15
Median	10	28	10
Maximum	208	131	136
Timing of Peak Human Transmission			
Mean	8/03	8/25	8/09
Median	8/01	8/30**	8/10
Earliest	6/22	8/14	6/27
Latest	8/30**	8/30**	8/30**
End of Season Egg Infection Rates			
Mean	0.90%	0.09%	0.38%
Median	0.70%	0.09%	0.28%
Maximum	6.6%	0.22%	3.4%

519 * As in the main paper, we do not report minimum values
520 **In these systems, the abundance of infected mosquitoes was still increasing at the end of the season. This
521 indicates that infection rates do not slow prior to the decline in mosquitoes at the end of the summer.

Table A7 Summary statistics for epidemiological metrics based on LHS analysis of the full dynamic model assuming a 5 month mosquito breeding season; all metrics beyond the first row are only calculated for the subset of simulations that gave infected mosquitoes

	Tree-hole Model	Tiger Model	Tree-hole and Tiger Model*
Parameter Sets with LAC Persistence	49%	0.47%	26%
End of Season Host Seroprevalence Rate			
Mean	89%	79%	86%
Median	99%	93%	98%
Maximum	100%	100%	100%
Mid-Season Host Seroprevalence Rate			
Mean	58%	8.3%	14%
Median	57%	5.8%	8.9%
Maximum	100%	37%	99%
Peak No. Infected Mosquitoes (ha^{-1})			
Mean	32	43	23
Median	20	38	15
Maximum	297	129	218
Peak Mosquito Infection Rate			
Mean	4.5%	1.4%	1.8%
Median	3.3%	1.2%	1.2%
Maximum	25%	3.5%	15%
Average Mosquito Infection Rate			
Mean	1.8%	0.43%	0.72%
Median	1.4%	0.39%	0.50%
Maximum	12%	1.2%	6.4%
Max. Human Transmission (mo^{-1}person^{-1}ha^{-1})			
Mean	16	57	14
Median	8.2	40	7.9
Maximum	208	259	244
Timing of Peak Human Transmission			
Mean	8/24	10/08	9/05
Median	8/18	10/13	9/01
Earliest	6/24	8/24	6/28
Latest	10/30**	10/30**	10/30**
End of Season Egg Infection Rates			
Mean	0.46%	0.06%	0.20%
Median	0.35%	0.05%	0.15%
Maximum	5.8%	0.19%	1.8%

* As in the main paper, we do not report minimum values

**In these systems, the abundance of infected mosquitoes was still increasing at the end of the season. This indicates that infection rates do not slow prior to the decline in mosquitoes at the end of the summer.

529   Appendix VII – Midwest LAC Cases

530   To examine LAC trends in the Midwest, we begin with data from Figure 1 of Leisnham and Juliano (66).

531   Figure A3 shows LAC cases per year, averaged over 1, 5, 10, and 20 year windows. From Figure A3, it

532   is clear that there has been a multi-decadal trend towards decreased LAC cases in the Midwest.

533
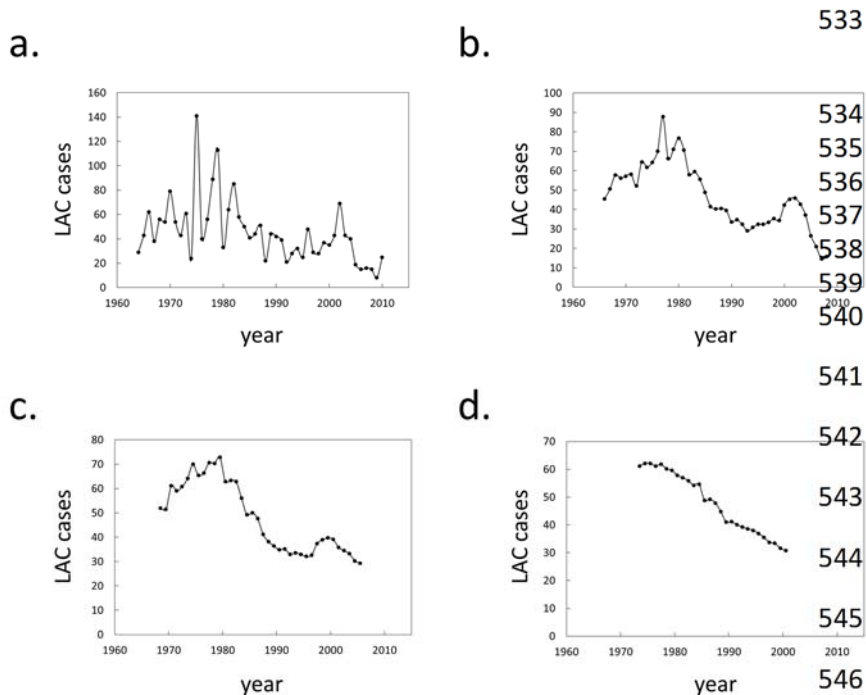
Figure A3 LAC cases per year, averaged over (a) 1 year, (b) 5 year, (c) 10 year and (d) 20 year windows. Original data are from (66) and sources within.

547

548   Notably, the tiger mosquito was first detected in Indiana, Illinois, and Ohio in 1986 (67, 68) and was

549   clearly established in southern portions of these states 10 years later (69, 70). Interestingly, this is also

550   the period over which the Midwest exhibited precipitous declines in LAC cases. Unlike LAC trends in

551   Appalachia, the long-term declines observed in the Midwest are consistent with general predictions from

552   our models.

553   Although the trends in Figure A3 suggest a declining LAC incidence rate in the Midwest coincident with

554   invasion of the tiger mosquito, we further explore this trend on a state-by-state basis. This is shown in

555   Figure A4, where we have separately considered (a) Appalachian states, (b) Midwest states that have been

556 invaded by the tiger mosquito and (c) Midwest states that have not been invaded by the tiger mosquito

557 using data from (71).
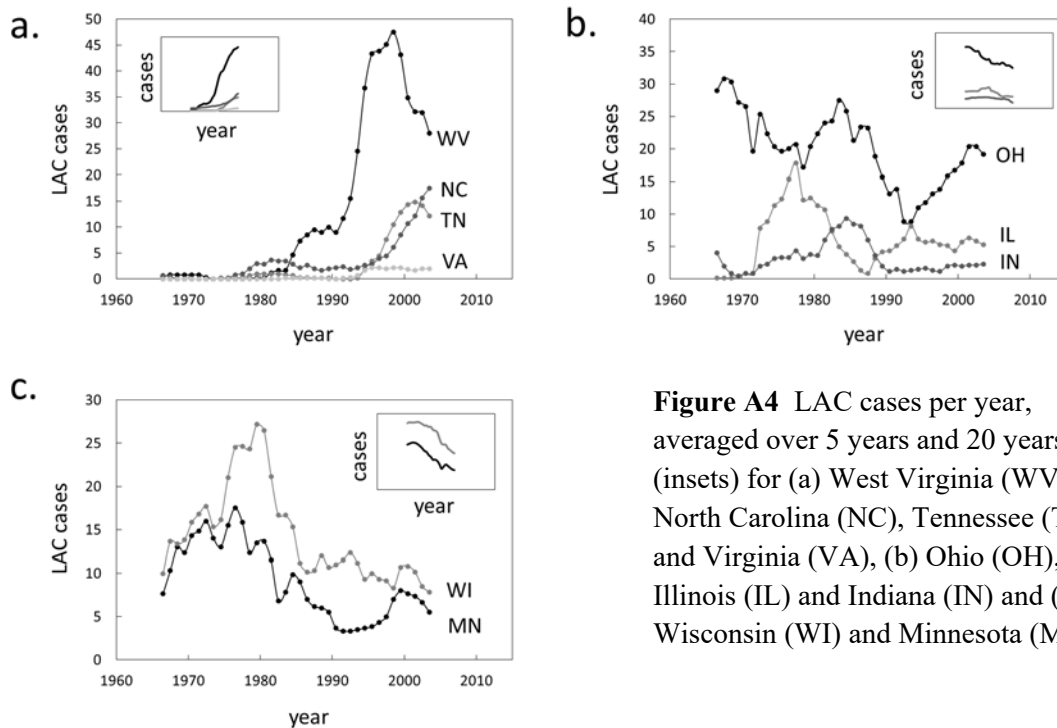
Figure A4 LAC cases per year, averaged over 5 years and 20 years (insets) for (a) West Virginia (WV), North Carolina (NC), Tennessee (TN) and Virginia (VA), (b) Ohio (OH), Illinois (IL) and Indiana (IN) and (c) Wisconsin (WI) and Minnesota (MN).

558

559 Based on Figure A4, we can draw several interesting conclusions. First, we see that North Carolina,

560 Tennessee, and to a lesser extent, Virginia did witness LAC increases coincident with the approximate

561 timing of tiger mosquito appearance in the region (69). However, the uptick in LAC in West Virginia

562 occurs well before the arrival of the tiger mosquito (69, 72). This supports our conclusion that other

563 factors, beyond the tiger mosquito, may be responsible for the upward trend in LAC in Appalachia.

564 (Notably, West Virginia was the state with the most dramatic increase in LAC between 1964 and 2005).

565 Second, we see that Ohio, Illinois and Indiana underwent LAC declines in the late 1980s. Again, this is

566 consistent with the arrival of the tiger mosquito (67, 68). However, it should be pointed out that these

567 declines, like the uptick in cases in West Virginia, appear to be part of larger trends that began somewhat

568 before tiger mosquito introduction. Furthermore, the observation of similar decreasing trends in

569 Wisconsin and Minnesota suggests that, like the upward trend in cases in Appalachia, the downward trend

570   in the Midwest may be relatively independent of the presence of the tiger mosquito. Specifically,

571   although the tiger mosquito was first detected in Minnesota in 1995 (69), recent surveys suggest that both

572   Wisconsin and Minnesota remain largely free of tiger mosquitoes (73, 74). Thus, while the lack of

573   increase in LAC cases in Ohio, Illinois and Indiana broadly support our conclusion that the tiger mosquito

574   is unlikely to amplify spread, it is unclear to what extent the decrease in LAC in the Midwest is driven by

575   invasion of the tiger mosquito versus other changes that might be simultaneously occurring.

576

577

578

579

580

581

582

583

584

585

586

587

588

589

590

591

592

593

594

595

Appendix VIII – Conditions Under Which Tiger Mosquitoes Enable LAC Spread

596

597 To further explore the role of tiger mosquitoes on LAC spread and persistence, we determine the

598 conditions under which tiger mosquitoes would be expected to benefit, rather than impede, LAC

599 transmission. Thresholds are shown in Figure A5. Notably, for tiger mosquitoes to enhance LAC

600 transmission, there would need to be extremely large increases in tiger mosquito biting rates on

601 chipmunks/squirrels (>5 fold), in tiger mosquito-to-chipmunk transmission rates (>15 fold), or in

602 chipmunk-to-tiger mosquito transmission rates (>5 fold), or else substantial decreases in tiger mosquito

603 competitive effects on tree-hole mosquitoes (>70% reduction).
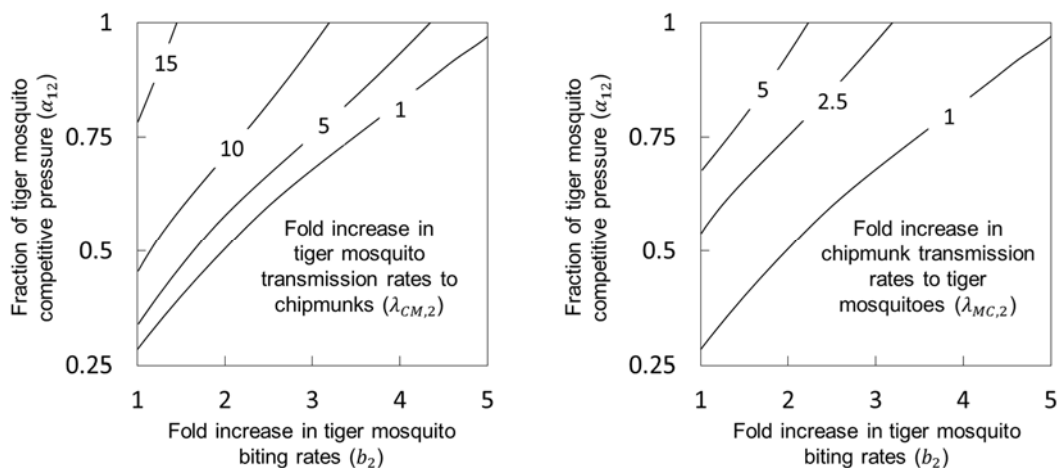
604

605

Figure A5 Fold increases in transmission rates (contour labels) and biting rates (x-
606 axis) and reductions in competitive pressure (y-axis) necessary to switch tiger
mosquitoes from preventing to enabling LAC spread as determined based on peak rates
607 of transmission to humans. All increases/decreases are relative to parameter values
reflecting the mid-points of the parameter ranges in Table A1.

608

609 These results suggest that, if tiger mosquitoes are, in fact, responsible for increasing LAC incidence rates

610 in Appalachia, then there are likely multiple unaccounted factors at play, including both strong niche

611 partitioning between tiger and tree-hole mosquitoes, as well as adaptation of LAC to the tiger mosquito

612 host such that transmission rates to and from the tiger mosquito are substantially higher than currently

613 available empirical estimates.

References for Supplemental Information

614

615 1.   Paulson SL, Grimstad PR. Replication and dissemination of La Crosse virus in the competent
616 vector *Aedes triseriatus* and the incompetent vector *Aedes hendersoni* and evidence for transovarial
617 transmission by *Aedes hendersoni* (*Diptera*: *Culicidae*). Journal of medical entomology. 1989;26(6):602-
618 9.
619 2.   Rust RS, Thompson WH, Matthews CG, Beaty BJ, Chun RW. Topical Review: La Crosse and
620 Other Forms of California Encephalitis. Journal of child neurology. 1999;14(1):1-14.
621 3.   Osorio JE, Godsey MS, Defoliart GR, Yuill TM. La Crosse viremias in white-tailed deer and
622 chipmunks exposed by injection or mosquito bite. The American journal of tropical medicine and
623 hygiene. 1996;54(4):338-42.
624 4.   Pantuwatana S, Thompson WH, Watts DM, Hanson RP. Experimental infection of chipmunks
625 and squirrels with La Crosse and Trivittatus viruses and biological transmission of La Crosse virus by
626 *Aedes triseriatus*. The American journal of tropical medicine and hygiene. 1972;21(4):476-81.
627 5.   Ksiazek T, Yuill T. Viremia and antibody response to La Crosse virus in sentinel gray squirrels
628 (Sciuris carolinensis) and chipmunks Tamias striatus). The American journal of tropical medicine and
629 hygiene. 1977;26(4):815-21.
630 6.   Wonham MJ, de-Camino-Beck T, Lewis MA. An epidemiological model for West Nile virus:
631 invasion analysis and control applications. Proceedings of the Royal Society of London B: Biological
632 Sciences. 2004;271(1538):501-7.
633 7.   Anderson RM, May RM. Infectious diseases of humans: Oxford university press Oxford; 1991.
634 8.   Watts D, Pantuwatana S, DeFoliart G, Yuill T, Thompson W. Transovarial transmission of
635 LaCrosse virus (California encephalitis group) in the mosquito, *Aedes triseriatus*. Science.
636 1973;182(4117):1140-1.
637 9.   Tesh RB, Gubler DJ. Laboratory studies of transovarial transmission of La Crosse and other
638 arboviruses by *Aedes albopictus* and *Culex fatigans*. The American journal of tropical medicine and
639 hygiene. 1975;24(5):876-80.
640 10.   Livdahl TP, Willey MS. Prospects for an invasion: competition between *Aedes albopictus* and
641 native *Aedes triseriatus*. Science. 1991;253(5016):189-91.
642 11.   Teng H-J, Apperson CS. Development and survival of immature Aedes albopictus and Aedes
643 triseriatus (Diptera: Culicidae) in the laboratory: effects of density, food, and competition on response to
644 temperature. Journal of medical entomology. 2000;37(1):40-52.
645 12.   Costanzo K, Muturi E, Montgomery A, Alto B. Effect of oral infection of La Crosse virus on
646 survival and fecundity of native *Ochlerotatus triseriatus* and invasive *Stegomyia albopicta*. Medical and
647 veterinary entomology. 2014;28(1):77-84.
648 13.   Cully JJ, Streit T, Heard P. Transmission of La Crosse virus by four strains of *Aedes albopictus* to
649 and from the eastern chipmunk (*Tamias striatus*). Journal of the American Mosquito Control Association.
650 1992;8(3):237-40.
651 14.   Patrican L, DeFoliart G, Yuill T. La Crosse viremias in juvenile, subadult and adult chipmunks
652 (*Tamias striatus*) following feeding by transovarially-infected *Aedes triseriatus*. The American journal of
653 tropical medicine and hygiene. 1985;34(3):596-602.
654 15.   Grimstad PR, Craig Jr GB, Ross QE, Yuill TM. *Aedes triseriatus* and LA crosse virus:
655 geographic variation in vector susceptibility and ability to transmit. The American journal of tropical
656 medicine and hygiene. 1977;26(5 Pt 1):990-6.
657 16.   Patrican L, DeFoliart G, Yuill T. Oral infection and transmission of La Crosse virus by an
658 enzootic strain of *Aedes triseriatus* feeding on chipmunks with a range of viremia levels. The American
659 journal of tropical medicine and hygiene. 1985;34(5):992-8.

660   17.   Paulson SL, Grimstad PR, Craig GB. Midgut and salivary gland barriers to La Crosse virus
661   dissemination in mosquitoes of the *Aedes triseriatus* group. Medical and veterinary entomology.
662   1989;3(2):113-23.
663   18.   Paulson SL, Hawley WA. Effect of body size on the vector competence of field and laboratory
664   populations of *Aedes triseriatus* for La Crosse virus. Journal of the American Mosquito Control
665   Association. 1991;7(2):170-5.
666   19.   Grimstad P, Kobayashi J, Zhang M, Craig Jr G. Recently introduced *Aedes albopictus* in the
667   United States: potential vector of La Crosse virus (Bunyaviridae: California serogroup). Journal of the
668   American Mosquito Control Association. 1989;5(3):422-7.
669   20.   Hughes MT, Gonzalez JA, Reagan KL, Blair CD, Beaty BJ. Comparative potential of *Aedes*
670   *triseriatus*, *Aedes albopictus*, and *Aedes aegypti* (*Diptera*: *Culicidae*) to transovarially transmit La Crosse
671   virus. Journal of medical entomology. 2006;43(4):757-61.
672   21.   Porter C, DeFoliart G, Miller B, Nemenyi P. Intervals to blood feeding following emergence and
673   oviposition in *Aedes triseriatus* (*Diptera*: *Culicidae*). Journal of medical entomology. 1986;23(2):222-4.
674   22.   Burkot T, DeFoliart G. Bloodmeal sources of *Aedes triseriatus* and*Aedes vexans* in a southern
675   Wisconsin forest endemic for La Crosse encephalitis virus. The American journal of tropical medicine
676   and hygiene. 1982;31(2):376-81.
677   23.   Haramis LD, Foster WA. Gonotrophic cycle duration, population age structure, and onset of
678   sugar feeding and insemination of *Aedes triseriatus* (*Diptera*: *Culicidae*). Journal of medical entomology.
679   1990;27(4):421-8.
680   24.   Walker ED, Copeland RS, Paulson SL, Munstermann LE. Adult survivorship, population density,
681   and body size in sympatric populations of *Aedes triseriatus* and *Aedes hendersoni* (*Diptera*: *Culicidae*).
682   Journal of medical entomology. 1987;24(4):485-93.
683   25.   Nasci RS. Differences in host choice between the sibling species of treehole mosquitoes *Aedes*
684   *triseriatus* and *Aedes hendersoni*. The American journal of tropical medicine and hygiene.
685   1982;31(2):411-5.
686   26.   Leisnham PT, Sala L, Juliano SA. Geographic variation in adult survival and reproductive tactics
687   of the mosquito *Aedes albopictus*. Journal of medical entomology. 2008;45(2):210-21.
688   27.   Niebylski M, Savage H, Nasci R, Craig Jr G. Blood hosts of *Aedes albopictus* in the United
689   States. Journal of the American Mosquito Control Association. 1994;10(3):447-50.
690   28.   Savage H, Niebylski M, Smith G, Mitchell C, Craig G. Host-feeding patterns of *Aedes albopictus*
691   (*Diptera*: *Culicidae*) at a temperate North American site. Journal of Medical Entomology. 1993;30(1):27-
692   34.
693   29.   Richards SL, Ponnusamy L, Unnasch TR, Hassan HK, Apperson CS. Host-feeding patterns of
694   *Aedes albopictus* (*Diptera*: *Culicidae*) in relation to availability of human and domestic animals in
695   suburban landscapes of central North Carolina. Journal of medical entomology. 2006;43(3):543-51.
696   30.   Delatte H, Gimonneau G, Triboire A, Fontenille D. Influence of temperature on immature
697   development, survival, longevity, fecundity, and gonotrophic cycles of *Aedes albopictus*, vector of
698   chikungunya and dengue in the Indian Ocean. Journal of medical entomology. 2009;46(1):33-41.
699   31.   Woodring J, Chandler LJ, Oray CT, McGaw MM, Blair CD, Beaty BJ. Short report: Diapause,
700   transovarial transmission, and filial infection rates in geographic strains of La Crosse virus-infected *Aedes*
701   *triseriatus*. The American journal of tropical medicine and hygiene. 1998;58(5):587-8.
702   32.   Beaty BJ, Thompson WH. Delineation of La Crosse virus in developmental stages of
703   transovarially infected *Aedes triseriatus*. The American journal of tropical medicine and hygiene.
704   1976;25(3):505-12.
705   33.   Borucki MK, Kempf BJ, Blitvich BJ, Blair CD, Beaty BJ. La Crosse virus: replication in
706   vertebrate and invertebrate hosts. Microbes and infection. 2002;4(3):341-50.
707   34.   Chandler LJ, Blair CD, Beaty BJ. La Crosse virus infection of *Aedes triseriatus* (*Diptera*:
708   *Culicidae*) ovaries before dissemination of virus from the midgut. Journal of medical entomology.
709   1998;35(4):567-72.

710 35.   Landry S, DeFoliart G, Hogg D. Adult body size and survivorship in a field population of *Aedes*
711 *triseriatus*. Journal of the American Mosquito Control Association. 1988;4(2):121-8.
712 36.   Sinsko MJ, Craig GB. Dynamics of an isolated population of *Aedes triseriatus* (*Diptera*:
713 *Culicidae*). I. Population size. Journal of Medical Entomology. 1979;15(2):89-98.
714 37.   Haramis LD, Foster WA. Survival and population density of *Aedes triseriatus* (*Diptera*:
715 *Culicidae*) in a woodlot in central Ohio, USA. Journal of medical entomology. 1983;20(4):391-8.
716 38.   Beier J, Berry W, Craig G. Horizontal distribution of adult *Aedes triseriatus* (*Diptera*: *Culicidae*)
717 in relation to habitat structure, oviposition, and other mosquito species. Journal of Medical Entomology.
718 1982;19(3):239-47.
719 39.   Brady OJ, Johansson MA, Guerra CA, Bhatt S, Golding N, Pigott DM, et al. Modelling adult
720 *Aedes aegypti* and *Aedes albopictus* survival at different temperatures in laboratory and field settings.
721 Parasit Vectors. 2013;6(1):351-62.
722 40.   Barrera R. Competition and resistance to starvation in larvae of container-inhabiting Aedes
723 mosquitoes. Ecological Entomology. 1996;21(2):117-27.
724 41.   Livdahl TP, Sugihara G. Non-linear interactions of populations and the importance of estimating
725 per capita rates of change. The Journal of Animal Ecology. 1984:573-80.
726 42.   Chmielewski M, Khatchikian C, Livdahl T. Estimating the per Capita Rate of Population Change:
727 How Well Do Life-History Surrogates Perform? Annals of the Entomological Society of America.
728 2010;103(5):734-41.
729 43.   Alto BW, Juliano SA. Temperature effects on the dynamics of *Aedes albopictus* (*Diptera*:
730 *Culicidae*) populations in the laboratory. Journal of medical entomology. 2001;38(4):548-56.
731 44.   Hanson SM, Craig GB. *Aedes albopictus* (*Diptera*: *Culicidae*) eggs: field survivorship during
732 northern Indiana winters. Journal of Medical Entomology. 1995;32(5):599-604.
733 45.   Pumpuni C, Walker E. Population size and survivorship of adult *Aedes triseriatus* in a scrap
734 tireyard in northern Indiana. Journal of the American Mosquito Control Association. 1989;5(2):166-72.
735 46.   Gauld L, Hanson R, Thompson W, Sinha S. Observations on a natural cycle of La Crosse virus
736 (California group) in Southwestern Wisconsin. The American journal of tropical medicine and hygiene.
737 1974;23(5):983-92.
738 47.   Flyger V, editor Urban gray squirrels—problems, management, and comparisons with forest
739 populations. Trans Northeast Fish Wildl Conf; 1970.
740 48.   Flyger V. Tree squirrels in urbanizing environments. Wildlife in an urbanizing environment Univ
741 Mass Coop Ext Serv, Amherst, MA. 1974:235-48.
742 49.   Manski DA, VanDruff LW, Flyger V. Activities of gray squirrels and people in a downtown
743 Washington, DC park: management implications: Wildlife Management Institute; 1981.
744 50.   Moulton DW, Thompson WH. California group virus infections in small, forest-dwelling
745 mammals of Wisconsin Some ecological considerations. The American journal of tropical medicine and
746 hygiene. 1971;20(3):474-82.
747 51.   Burkot T, DeFoliart G. Bloodmeal sources of Aedes triseriatus and Aedes vexans in a southern
748 Wisconsin forest endemic for La Crosse encephalitis virus. The American journal of tropical medicine
749 and hygiene. 1982;31(2):376-81.
750 52.   Farjana T, Tuno N. Multiple blood feeding and host-seeking behavior in Aedes aegypti and
751 Aedes albopictus (Diptera: Culicidae). Journal of medical entomology. 2013;50(4):838-46.
752 53.   Livdahl TP, Edgerly JS. Egg hatching inhibition: field evidence for population regulation in a
753 treehole mosquito. Ecological entomology. 1987;12(4):395-9.
754 54.   Livdahl TP. Interspecific interactions and the rK continuum: laboratory comparisons of
755 geographic strains of Aedes triseriatus. Oikos. 1984:193-202.
756 55.   Kaplan L, Kendell D, Robertson D, Livdahl T, Khatchikian C. Aedes aegypti and Aedes
757 albopictus in Bermuda: extinction, invasion, invasion and extinction. Biological Invasions.
758 2010;12(9):3277-88.
759 56.   Juliano SA. Coexistence, exclusion, or neutrality? A meta-analysis of competition between Aedes
760 albopictus and resident mosquitoes. Israel journal of ecology & evolution. 2010;56(3-4):325-51.

761 57.   DeFoliart GR. *Aedes triseriatus*: vector biology in relationship to the persistence of La Crosse
762 virus in endemic foci. Progress in clinical and biological research. 1983;123:89.
763 58.   Carrieri M, Angelini P, Venturelli C, Maccagnani B, Bellini R. Aedes albopictus (Diptera:
764 Culicidae) population size survey in the 2007 Chikungunya outbreak area in Italy. II: estimating epidemic
765 thresholds. Journal of medical entomology. 2012;49(2):388-99.
766 59.   Cianci D, Van Den Broek J, Caputo B, Marini F, Della Torre A, Heesterbeek H, et al. Estimating
767 Mosquito Population Size From Mark–Release–Recapture Data. Journal of medical entomology.
768 2013;50(3):533-42.
769 60.   Gouagna LC, Dehecq J-S, Fontenille D, Dumont Y, Boyer S. Seasonal variation in size estimates
770 of Aedes albopictus population based on standard Mark-release-recapture experiments in an urban area on
771 Reunion Island. Acta tropica. 2015.
772 61.   Parker TS, Nilon CH. Gray squirrel density, habitat suitability, and behavior in urban parks.
773 Urban Ecosystems. 2008;11(3):243-55.
774 62.   Van den Driessche P, Watmough J. Reproduction numbers and sub-threshold endemic equilibria
775 for compartmental models of disease transmission. Mathematical biosciences. 2002;180(1):29-48.
776 63.   Hartemink N, Randolph S, Davis S, Heesterbeek J. The Basic Reproduction Number for Complex
777 Disease Systems: Defining R0 for Tick-Borne Infections. The American Naturalist. 2008;171(6):743-54.
778 64.   Mailleret L, Lemesle V. A note on semi-discrete modelling in the life sciences. Philosophical
779 Transactions of the Royal Society of London A: Mathematical, Physical and Engineering Sciences.
780 2009;367(1908):4779-99.
781 65.   Blower SM, Dowlatabadi H. Sensitivity and uncertainty analysis of complex models of disease
782 transmission: an HIV model, as an example. International Statistical Review/Revue Internationale de
783 Statistique. 1994:229-43.
784 66.   Leisnham PT, Juliano SA. Impacts of climate, land use, and biological invasion on the ecology of
785 immature *Aedes* mosquitoes: implications for La Crosse emergence. Ecohealth. 2012;9(2):217-28.
786 67.   Moore CG, Francy D, Eliason D, Monath T. Aedes albopictus in the United States: rapid spread
787 of a potential disease vector. Journal of the American Mosquito Control Association. 1988;4(3):356-61.
788 68.   Wesson D, Hawley W, Craig Jr GB. Status of Aedes albopictus in the midwest: La Crosse belt
789 distribution, 1988. Proceedings of the Illinois Mosquito and Vector Control Association. 1990;1:11-5.
790 69.   Moore CG, Mitchell CJ. Aedes albopictus in the United States: ten-year presence and public
791 health implications. Emerging infectious diseases. 1997;3(3):329.
792 70.   Moore CG. Aedes albopictus in the United States: current status and prospects for further spread.
793 Journal of the American Mosquito Control Association. 1999;15(2):221-7.
794 71.   Control CfD, Prevention. Confirmed and Probable California Serogroup Viral (mainly La Crosse)
795 Encephalitis Cases, Human, United States, 1964–2005. Centers for Disease Control and Prevention,
796 Atlanta, GA. 2005.
797 72.   Control CfD. La Crosse encephalitis in West Virginia. MMWR Morbidity and mortality weekly
798 report. 1988;37(5):79.
799 73.   Hahn MB, Eisen RJ, Eisen L, Boegler KA, Moore CG, McAllister J, et al. Reported Distribution
800 of Aedes (Stegomyia) aegypti and Aedes (Stegomyia) albopictus in the United States, 1995-2016
801 (Diptera: Culicidae). Journal of Medical Entomology. 2016:tjw072.
802 74.   Prevention CfDCa. Geographic Distribution http://www.cdc.gov/zika/vector/range.html2016
803 [7/29/2016].

804